Supplemental Material:

Rice Cellulose SynthaseA8 Plant-Conserved Region is a coiled-coil at the catalytic core entrance

Phillip S. Rushton[a], Anna T. Olek[b], Lee Makowski[c], John Badger[d], C. Nicklaus Steussy[a], Nicholas C. Carpita[a,b,e], and Cynthia V. Stauffacher[a,e,f]

[a]Department of Biological Sciences, Purdue University, Hockmeyer Hall of Structural Biology, 240 S. Martin Jischke Dr., West Lafayette, IN 47907

[b]Department of Botany & Plant Pathology, Purdue University, 915 West State Street, West Lafayette, IN 47907

[c]Departments of Bioengineering and Chemistry and Chemical Biology, Northeastern University, 360 Huntington Avenue, Boston, MA 02115

[d]DeltaG Technologies, 4360 Benhurst Avenue, San Diego, CA 92122

[e]Bindley Bioscience Center, Purdue University, 1203 West State Street, West Lafayette, IN 47907

[f]Purdue Center for Cancer Research, Purdue University, 201 S. University St., West Lafayette, IN 47907

One Sentence Summary: The crystal structure of a rice CesA8 plant-conserved region (P-CR) has been solved to 2.4Å resolution and docked to a model of the catalytic domain of CesA8 using SAXS molecular envelopes.

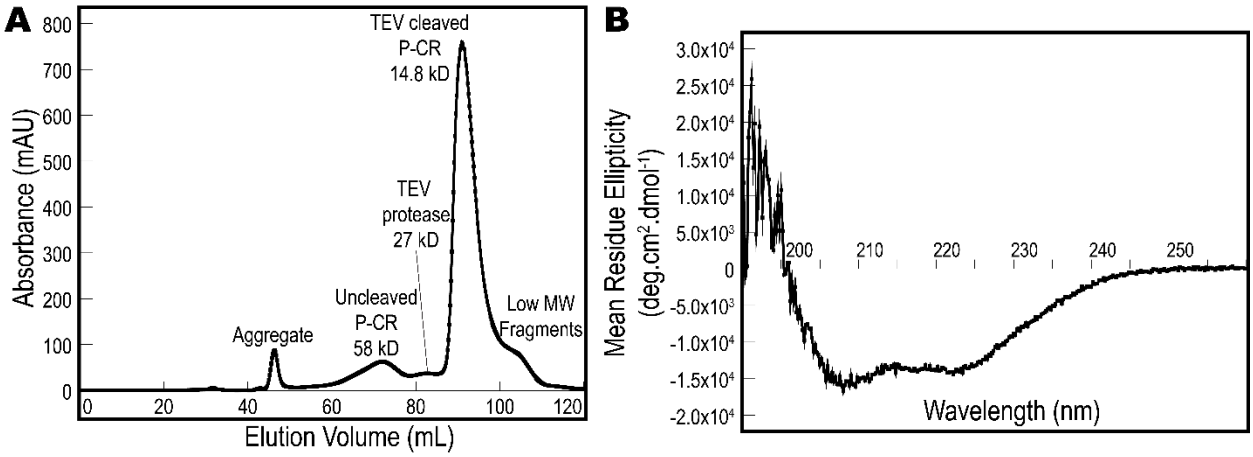

Supplemental Figure S1. P-CR Secondary Structure and Apparent Molecular Weight Analysis.

(**A**) The SEC chromatogram of the TEV protease cleaved P-CR showed a single well-formed elution peak corresponding to the TEV cleaved P-CR, along with other small contaminate peaks. (**B**) The mean residue ellipticity of the P-CR between 195-260 nm is consistent with a primarily α-helical secondary structure, characterized by the strong negative peaks at 208 and 222 nm. Analysis of the spectra shows 59% α-helical, 8% β-strand and 33% random coil secondary structure using the K2D deconvolution algorithm (Andrade et al., 1993) on the DichroWeb server (Whitmore and Wallace, 2004).

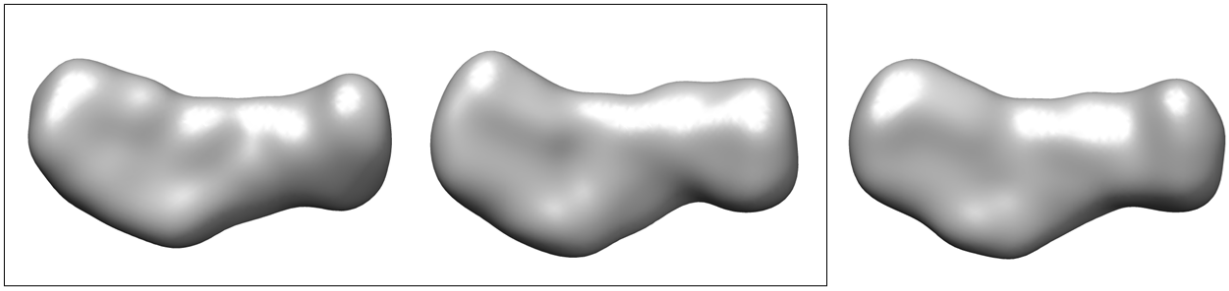

Supplemental Figure S2. Reconstructing the P-CR SAXS Molecular Envelope. The final SAXS reconstruction of the P-CR molecular envelope was based on the average of 40 dummy residue models obtained with GASBOR with a mean NSD=1.35. Two independent sets of 20 models were selected using even and odd serial numbers from the set of 40 models. The reconstructions from these two disparate subsets of models are similar (boxed reconstructions), indicating that the reconstruction based on all 40 bead models (right) is a reliable average.

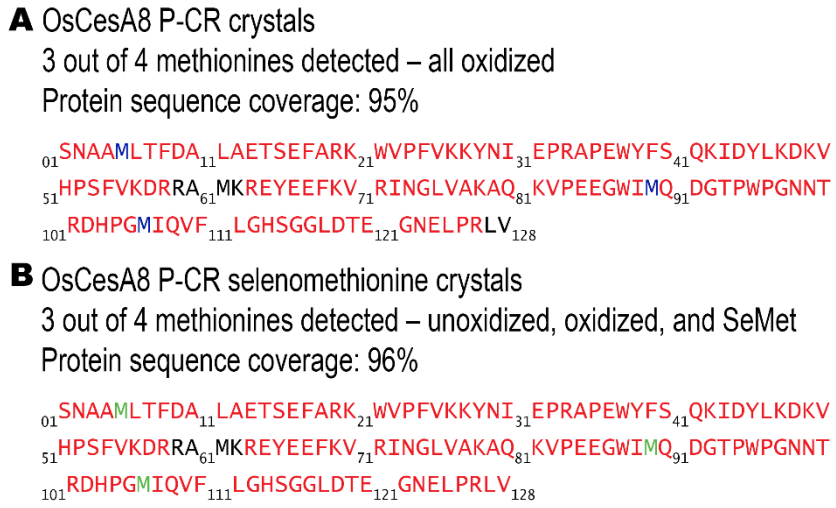

Supplemental Figure S3. Sequence Coverage for Mass Spectrometry Data of OsCesA8 P-CR Crystals.

OsCesA8 P-CR crystals washed in reservoir solution were run on SDS-PAGE and the single bands produced were submitted for mass spectrometry proteomic analysis. Matching peptide fragments are shown in red, undetected residues are shown in black. (**A**) OsCesA8 P-CR crystals showed excellent coverage over the entire OsCesA8 P-CR sequence. 3 of 4 methionines were oxidized (blue). (**B**) OsCesA8 P-CR selenomethionine crystals also showed excellent coverage over the entire OsCesA8 P-CR sequence but still could not detect the 4th methionine present in the RAMK peptide fragment. In this case the same 3 of 4 methionines as in **A** were shown to be a mixture of oxidized methionine, unoxidized methionine and selenomethionine substituted (green).

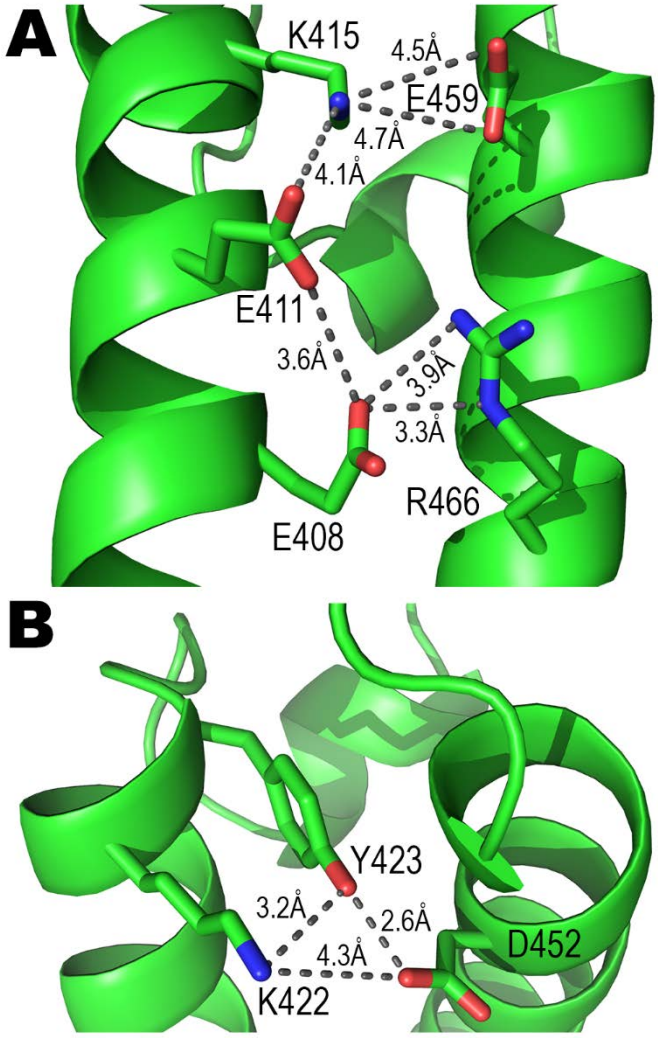

Supplemental Figure S4. Electrostatic Interactions Between Coiled-Coil α-Helices (HX1 and HX2).

Several weak hydrogen bonds between helices are found on the solvent face of the P-CR, defined as the opposite side as the interactions between loop region and the coiled-coil hydrophobic core. (**A**) Near the N- and C- termini of the coiled-coil Glu_{411} bridges Lys_{415} and Glu_{408} on HX1, which then form interactions between the helices with Glu_{459} and Arg_{466}, respectively. (**B**) At the opposite end, closer to the loop region, the hydroxyls of Tyr_{423} and Asp_{452} bridge with Lys_{422} in a three center interaction.

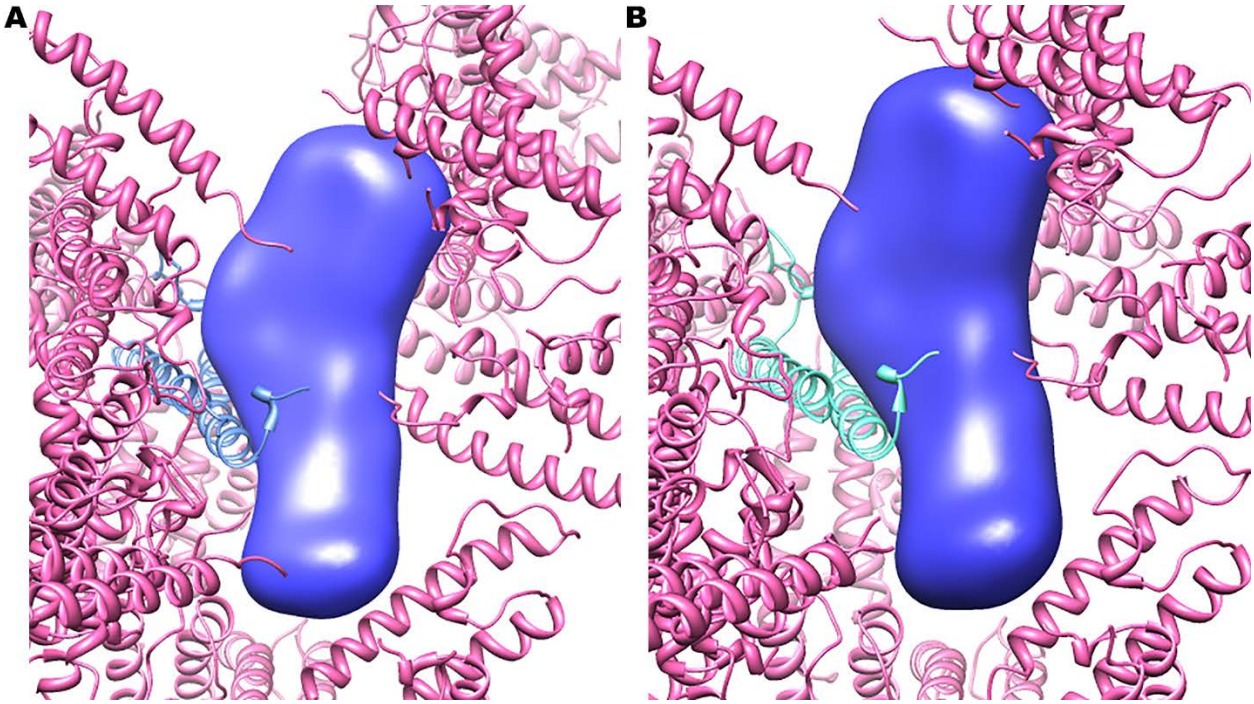

Supplemental Figure S5. The P-CR SAXS Molecular Envelope Fit into the P-CR Crystal Lattice.

The SAXS envelope (blue envelope) packs neatly into the crystal cell lattice when overlaid on either of the independent molecules in the crystal cell. (**A**) Fit over molecule A shown with molecule B (blue Cα trace) and molecules related by crystallographic symmetry (pink). (**B**) Fit over molecule B obtained by applying the NCS symmetry, shown with molecule A (cyan) and molecules related by crystallographic symmetry (pink). Full symmetry expansion of the SAXS envelope in the crystal lattice showed that there are no significant overlaps between these molecular volumes within the resolution of the SAXS data.

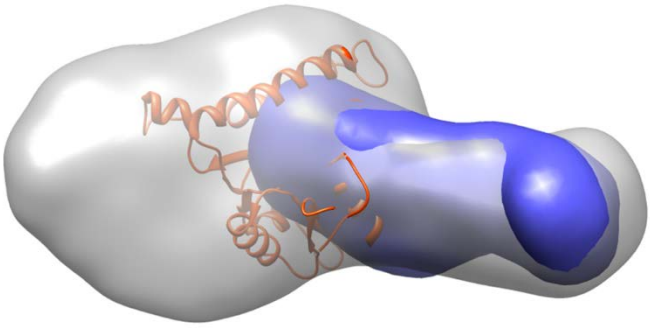

Supplemental Figure S6. Alternative Fit of the P-CR into CesA8 CatD Molecular Envelope.

Docking trials in which the P-CR volume (blue surface) is placed so as to fill the smaller domain in the CesA8 CatD volume (grey surface), previously assigned to the CSR (Olek et al., 2014). This placement results in the P-CR protruding far into the central region occupied by the catalytic core (orange ribbon, showing a representative pose with the model based on the chain trace of BcsA).

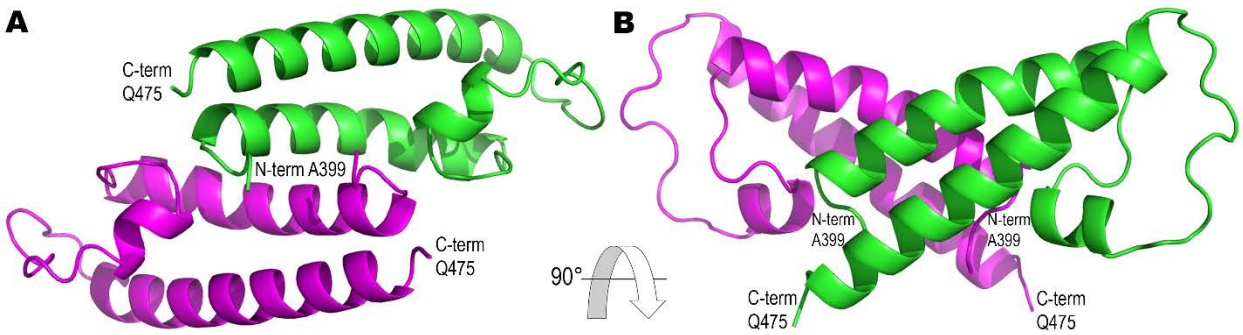

Supplemental Figure S7. The Noncrystallographic Dimer of the P-CR Structure. The asymmetric unit of the F23 shows two identical P-CR monomers (green and purple, respectively) interacting across a two-fold symmetrical contact between coiled-coil helix HX1 for each monomer. The LP region and upper portions of the coiled-coil helices, distal to the N and C terminus of each monomer, extend beyond the N-terminal junction of the other P-CR monomer with the 1st signature sequence containing the 1st catalytic Asp residue. In the context of the full-length protein this would cause extensive clashes with the catalytic core, and the structural differences between the CesAs and BcsA catalytic cores required to accommodate this dimer appear unlikely given the high sequence conservation of the catalytic core.

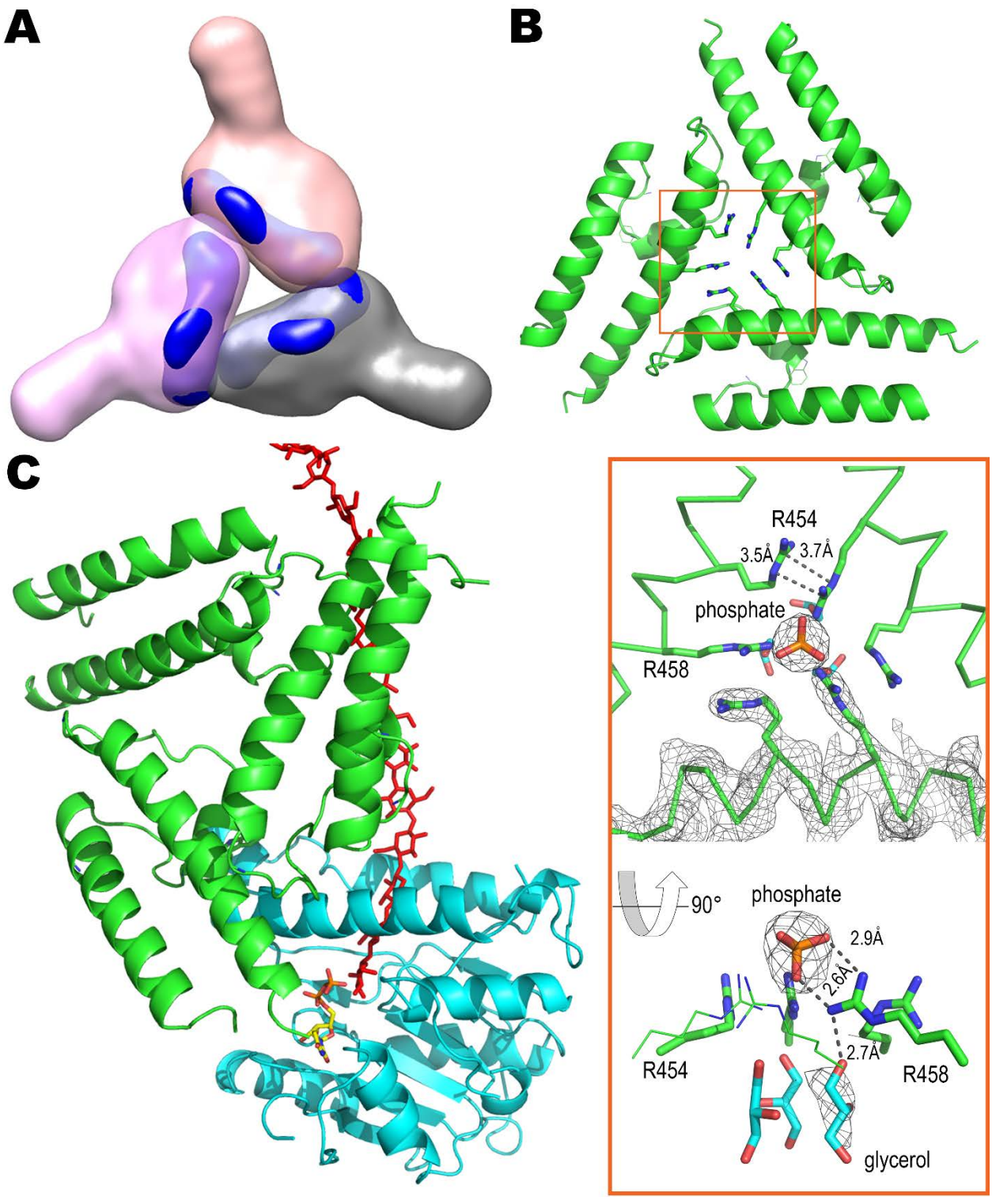
A
B
C
R454
3.5Å
3.7Å
phosphate
R458
90°
phosphate
2.9Å
2.6Å
2.7Å
R454
R458
glycerol

Supplemental Figure S8. Constructing a P-CR Trimer from SAXS and Crystallographic Data.

(**A**) The P-CR and subsequent best fit CesA8 CatD SAXS molecular envelopes (this work, Olek et al., 2014) can be aligned to a three-fold axis to approximate the overall SAXS envelope of the AtCesA1 catalytic domain trimer (Vandavasi et al., 2016). In this configuration the contacts are mediated by the P-CR. (**B**) Using the best fit alignment of the crystallographic structure of the P-CR to the SAXS generated model, the trimeric contacts overlay those around the three-fold in the crystal. Arg_{454} and Arg_{458} participate in an unusual stacked interaction, stabilized by a phosphate ion (insert). (**C**) Taking the best model of the P-CR and CatD based on our combined SAXS and crystallographic evidence and superimposing this on the BcsA catalytic core (Morgan et al., 2013) gave the model first shown in Figure 5D. Only the catalytic core (blue) and P-CR (green) of CesA8 are shown here. Adding the trimeric P-CR interaction to this model (three green P-CR domains) would require the other two P-CRs to protrude into the membrane, indicating this trimeric model is unlikely to be a biologically relevant structure.

SUPPLEMENTAL REFERENCES

Andrade, M.A., Chacón, P., Merelo, J.J., and Morán, F. (1993). Evaluation of secondary structure of proteins from UV circular dichroism spectra using an unsupervised learning neural network. Protein Eng. **6**: 383-390.

Grigoryan, G., Keating, A.E. (2008). Structural specificity in coiled-coil interactions. Curr. Opin. Struct. Biol. **18:** 477-483.

Morgan, J.L., Strumillo, J., and Zimmer, J. (2013). Crystallographic snapshot of cellulose synthesis and membrane translocation. Nature **493**: 181-186.

Olek, A.T., Rayon, C.J., Makowski, L., Ciesielski, P., Badger, J., Paul, L.N., Kim, H.-R., Ghosh, S., Kihara, D., Crowley, M., et al. (2014) The structure of the catalytic domain of a plant cellulose synthase and its assembly into dimers. Plant Cell **26**:2996-3009.

Vandavasi, V.G., Putnam, D.K., Zhang, Q., Petridis, L., Heller, W.T., Nixon, B.T., Haigler, C.H., Kalluri, U., Coates, L., Langan, P., et al. (2016) A structural study of CESA1 catalytic domain of Arabidopsis cellulose synthesis complex: Evidence for CESA trimers. Plant Physiol. **170:** 123-135.

Whitmore, L., and Wallace, B.A. (2004). Dichroweb, an online server for protein secondary structure analyses from circular dichroism spectroscopic data. Nucleic Acids Res. **32:** W668-W673.